DALTON

Biomimetic control of iron oxide and hydroxide phases in the iron oxalate system *

Michel Molinier, Daniel J. Price, Paul T. Wood and Annie K. Powell

School of Chemical Sciences, UEA, Norwich, UK NR4 7TJ

The syntheses of mineral phases of iron formed under hydrolytic conditions have been studied using ambient and hydrothermal methods in the presence and absence of the oxalate (ox) template. A systematic survey of experimental parameters revealed how the oxolate template can influence crystal morphology, iron oxidation state and the nature of the phase formed. In addition to observing biomimetic control over crystal morphology of magnetite, two iron(II) hydrolytic oxalate phases were observed, humboldtine, $Fe^{II}(ox)(H_2O)_2$, and the new phase, $Fe^{II}_2(ox)(OH)_2$, which was identified by single-crystal X-ray diffraction.

As has been pointed out by workers such as Mann and Ozin,[1–3] the remarkable control over the inorganic phase effected by organisms in the production and fashioning of mineralised deposits acting, for example, as bones, teeth, shells, and sensors is an achievement to which material scientists aspire. It is believed that the particular success of organisms in producing tailored mineralised species, often of unusual and metastable phases, is a result of the clever use of templates, such as protein side-chains and collagen, to reduce surface energy terms and favour nucleation and crystal growth of solid phases. These templates can also direct growth, either by providing physical barriers or by promoting or inhibiting growth in specified crystallographic directions. Although this is easy to appreciate intuitively, the actual means by which such templates act is hard to ascertain. One problem is that in condensed phases small amounts of the templating matrix will be difficult to detect making it hard to discover to what extent the matrix becomes incorporated in the mineral. However, experiments performed *in vitro* with a variety of growing mineral phases, such as calcite and aragonite (polymorphs of $CaCO_3$), suggest that growth can be inhibited or enhanced by the presence of groups such as carboxylates, which can substitute for the carbonate moieties at the growing surface of the mineral.[4] Additionally, the use of a variety of surfactants to mimic the action of templates in influencing crystal phase and architecture has produced structures displaying some aspects of the intricate frameworks and forms observed in Nature.[5,6]

Biomineralisation in general can be said to take place in aqueous environments, therefore the precipitation of mineralised deposits from water is of relevance. In the case of hydrolysing species such as metal ions the water can become an integral part of the solid phase in the form of oxide and hydroxide bridging anionic units as well as neutral co-ordinated water molecules and we term these structures hydrolytic phases. The presence of other co-ordinating species can affect the nature of the phase formed. We have been exploring the parameters which can influence crystal form and phase with the specific goal of gaining a deeper understanding of the way in which templating species can alter nucleation and crystal growth in the production of tailored materials. Overall for a metal ion, M^{n+}, in the presence of some templating species, L^{m-}, in water the hydrolysis of the metal ion to yield the hydroxide $M(OH)_n$, which can then evolve into other oxyhydroxide and oxide phases, can be modified by L and the various species possible can be summarised according to Scheme 1 where *a* and *b* are the charges on the metal/ligand species which will depend on the

$$[ML_z]^a + H_2O \rightleftharpoons [M_yL_zO_p(OH)_q(H_2O)_r]^b \rightleftharpoons M(OH)_n$$

Scheme 1

relative proportions of *m*, *n*, *y*, *z*, *p*, *q* and *r*. Further influences on this are the availability of other redox states of the metal, the effect of the templating ligand on redox state, the presence of other ionic species such as chloride, carbonate, phosphate, *etc*. which can affect ionic strength and also act as growth promoters or inhibitors, local pH gradients and the relative proportions of M, L and H_2O.

In our programme of research we have tried to address the factors which are important in the production of iron biominerals. All classes of biomineral function for iron oxyhydroxides and oxides are represented[7] and include structural deposits such as the radular teeth of various molluscs made of goethite, α-FeO(OH), lepidocrocite, γ-FeO(OH), and magnetite, Fe_3O_4, sensors made of magnetic iron oxide particles, usually magnetite, in magnetotactic bacteria, birds, bees, salmon, *etc.* and metal-ion regulation, as demonstrated by iron storage in ferritin probably in the form of ferrihydrite 'Fe(OH)$_3$' or $5Fe_2O_3{\cdot}9H_2O$.

Previously we have shown how tetradentate templating ligands can be used to modify the hydrolysis of Fe^{III} to trap portions of the brucite, $M(OH)_2$, structure under ambient synthetic conditions.[8,9] We have extended these studies to other metals and templating ligands using both ambient and hydrothermal synthetic methods.[10–13] Our rationale in using hydrothermal syntheses is the recognition that Nature is able to effect chemical reactions not accessible to us under similar conditions *in vitro*, such as the fixation of dinitrogen to give ammonia, which *Azotobacter* achieves in high yields at room temperature and pressure whereas we need to resort to the Haber–Bosch process using conditions of 200 atm (atm = 101 325 Pa) and 400 °C with yields of less than 20%. Thus the use of more extreme synthetic conditions than found in Nature offers the possibility of stabilising biomimetic mineralised phases which might not be achievable under ambient conditions *in vitro.*

We report here on the reactions of iron-(II) and -(III) starting materials in aqueous systems under a variety of pH, temperature and pressure conditions in the presence and absence of the oxalate (ox) template to produce the hydrolytic iron minerals magnetite, $Fe^{II}Fe^{III}_2O_4$, haematite, α-$Fe^{III}_2O_3$, humboldtine, $Fe^{II}(ox)(H_2O)_2$, and the new iron synthetic hydroxooxalate mineral $Fe^{II}_2(ox)(OH)_2$ and consider the influences of the oxalate template on the phase, oxidation state and crystal morphology.

Experimental

Hydrothermal reactions were carried out in Teflon-lined autoclaves with a capacity of 23 cm^3. All reactions were performed

* Based on the presentation given at Dalton Discussion No. 2, 2nd–5th September 1997, University of East Anglia, UK.

Table 1 The effect of base on the products of the hydrothermal syntheses

Iron salt (mmol)	Additional component(s) (mmol)	Base (mmol)	Temperature (°C)	Duration (h)	Product
$FeCl_3$ (1.1)	KCl (23.5)	KOH (3.0)	200	23	Haematite
$FeCl_3$ (1.1)	KCl (22.3)	KOH (3.1)	200	95	Haematitie
$FeCl_3$ (1.1)	$K_2C_2O_4$ (1.2)	KOH (3.7)	200	16	Haematitie
$FeCl_3$ (1.1)	$K_2C_2O_4$ (1.1)	KOH (3.7)	200	63	Haematitie
$FeCl_2$ (1.2)	KCl (22.3)	KOH (2.2)	200	20	Magnetite
$FeCl_2$ (1.1)	KCl (22.1)	KOH (1.9)	200	94	Magnetite
$FeCl_2$ (1.1)	$K_2C_2O_4$ (1.1)	KOH (2.7)	200	22	Magnetite
$FeCl_2$ (1.1)	$K_2C_2O_4$ (1.1)	KOH (2.7)	200	118	Magnetite
$FeCl_2$ (1.5)	$Na_2C_2O_4$ (2.9)	—	180	96	$Fe(ox)(H_2O)_2$ [a]
$FeCl_2$ (1.6)	$Na_2C_2O_4$ (3.2)	dabco [b] (3.1)	180	19	Magnetite
Fe_2O_3 (2.0)	$H_2C_2O_4$ (2.6)	—	220	40	$Fe(ox)(H_2O)_2$
$FeCl_3$ (1.1)	$Na_2C_3O_5$ [c] (0.9) +NaCl (23.3)	—	160	68	$Fe(ox)(H_2O)_2$

[a] Magnetite was observed as a trace impurity. [b] dabco is 1,4-diazabicyclo[2.2.2]octane. [c] Oxomalonic acid disodium salt.

in distilled water (10 cm^3) between 160 and 240 °C under autogenous pressure. After reaction autoclaves were allowed to cool slowly to room temperature over 3–4 h. A number of reactions were performed under ambient conditions for comparison. No special attempts to exclude oxygen were made for both hydrothermal and ambient reactions.

The solid products were characterised by scanning electron microscopy on a Hitachi S-800 instrument, infrared spectroscopy on a Nicolet 410 FTIR spectrometer as KBr discs from 4000 to 400 cm^{-1} at a resolution of 4 cm^{-1}, X-ray powder diffraction on a Philips PW1710 instrument using Co-Kα radiation with samples held in place on Sellotape and single-crystal X-ray diffraction on a Rigaku AFC7R diffractometer. Samples of magnetite were further identified using a bar magnet.

Syntheses

The interaction of iron-(II) and -(III) starting salts under hydrolysing conditions in the presence and absence of oxalate was studied using both ambient and hydrothermal reactions. The results of the hydrothermal studies are presented in Tables 1 and 2. The optimum synthetic conditions for the two iron(II) oxalate phases use hydrothermal methods and iron(III) chloride hexahydrate as starting iron source as detailed below.

$Fe_2(ox)_2(OH)_2$ 1. The compound $FeCl_3 \cdot 6H_2O$ (0.303 g, 1.12 mmol) was dissolved in distilled water (10 cm^3) and left to stand for 20 min. Solid $Na_2(C_2O_4)$ (0.304 g, 2.27 mmol) was added with stirring. The mixture was placed in the Teflon liner of an autoclave which was then sealed and heated to 240 °C for 16 h. It was allowed to cool to room temperature over 4 h and the brown-orange microcrystalline product filtered off and allowed to air dry. Small quantities of magnetite were separated using a bar magnet which was drawn through the bulk leaving an essentially pure product (from satisfactory elemental analysis) $Fe_2(ox)(OH)_2$ in a yield of 0.113 g, 86% based on iron. IR 3415s, 2200w (br), 1615s, 1361s, 1316s, 953m, 830m, 782m and 505s cm^{-1}.

$Fe(ox)(H_2O)_2$ 2. The same procedure as for the preparation of compound **1** was followed except that the autoclave was heated only to 160 °C. Traces of magnetite in the final product were again separated using a bar magnet to give a final yield of $Fe(ox)(H_2O)_2$ of 0.149 g, 68%. IR 3349vs (br), 2181w (br), 1623vs, 1361s, 1317s, 822m, 721m, 529s (br) and 493s cm^{-1}.

Crystallography

Crystal data for $Fe_2(ox)(OH)_2$. $CHFeO_3$, $M = 116.87$, monoclinic, space group $P2_1/c$, $a = 5.9270(10)$, $b = 5.5350(10)$, $c = 7.2740(10)$ Å, $\beta = 90.59(3)°$, $U = 238.62(7)$ $Å^3$, $Z = 4$, $D_c = 3.253$ g cm^{-3}, μ(Mo-Kα) = 6.034 mm^{-1}, $F(000) = 228$, 420 unique reflections were collected of which 352 had $F > 4\sigma(F)$, $5 < 2\theta < 50°$ graphite-monochromated Mo-Kα radiation ($\lambda = 0.710\ 73$ Å).

An empirical absorption correction based on ψ scans was applied using TEXSAN software,[14] minimum-maximum transmission factors 0.9153–1.000, crystal description, orange needle 0.30 × 0.03 × 0.03 mm, ω–2θ scans, $T = 293$ K. A correction for Lorentz-polarisation effects was applied and the structure was solved by direct methods.[15] The hydrogen atom was located from a difference map and refined isotropically without constraints; all other atoms were refined anisotropically using full-matrix least squares on $|F^2|$ using SHELXL 93 software.[16] 51 Parameters refined, $R1 = 0.019$, $wR2$ (all data) = 0.053, weighting scheme $w = 1/[\Sigma^2(F_o^2) + (0.0198P)^2 + 0.18P]$, where $P = [\max(F_o^2, 0) + 2F_c^2]/3$, $S = 1.151$, $\xi = 0.011(3)$, maximum residual electron density (largest electron hole) = 0.367 (−0.420) e $Å^{-3}$.

CCDC reference number 186/674.

Results and Discussion

Ambient reactions

To aid the interpretation of the results of the hydrothermal synthesis the effect of oxalate and base on solutions of iron-(II) and -(III) chlorides was studied. In all cases immediate precipitates form which precludes the measurement of meaningful pH values. When base is added to a solution of $FeCl_3 \cdot 6H_2O$ an orange-brown precipitate forms of 'Fe(OH)$_3$'. However if aqueous $FeCl_2 \cdot 4H_2O$ is treated with base a precipitate of 'green rust' forms which is slowly air oxidised to give 'amorphous magnetite' as has been observed previously.[17,18] When base is added to a 2:1 solution of $FeCl_3 \cdot 6H_2O$ and $FeCl_2 \cdot 4H_2O$ an amorphous magnetic black precipitate is formed. Aqueous solutions of $FeCl_2 \cdot 4H_2O$ (0.12 to 0.09 M) with 1, 2 and 4 equivalents of potassium oxalate (0.13 to 0.38 M) were treated with 1, 2 and 4 equivalents of aqueous potassium hydroxide. With 1 and 2 equivalents of base a dark green precipitate formed which was more rapidly air oxidised to the amorphous magnetic black precipitate than without the oxalate present. For solutions containing only Fe^{II} and oxalate the previously reported mineral humboldtine, $Fe(ox)(H_2O)_2$ **2**,[19,20] forms.

Hydrothermal reactions

The product of hydrothermal reactions of iron(II) chloride and oxalate (Table 1) in the absence of any base is yellow needles of the previously reported mineral phase, humboldtine $Fe(ox)(H_2O)_2$ **2**.[19,20] This always forms with trace amounts of magnetite present, which must be a result of the partial oxidation of the iron through hydrolytic reactions. When the amount of base used is increased the amount of magnetite observed

Table 2 Hydrothermal reactions with iron(III) and oxalate in the absence of base

	Amount of reagent (mmol)				
Reaction	$FeCl_3$	$Na_2C_2O_4$	Temperature (°C)	Duration (h)	Products
(i)	1.10	2.16	160	19	$Fe(ox)(H_2O)_2$
(ii)	1.07	2.25	200	19	$Fe(ox)(H_2O)_2$*
(iii)	1.07	2.16	240	19	Colourless crystals*
(iv)	1.23	2.52	160	16	$Fe(ox)(H_2O)_2$
(v)	1.19	2.19	200	16	$Fe(ox)(H_2O)_2$*
(vi)	1.16	2.27	240	16	$Fe_2(ox)(OH)_2$*

In reactions (i) to (iii) sodium oxalate was dissolved first, then solid iron(III) chloride was added. The identity of the colourless crystals in reaction (iii) has yet to be established. In reactions (iv) to (vi) the iron salt was dissolved first, allowed to stand for 20 min, then solid sodium oxalate added.
* Magnetite was observed as a trace impurity.

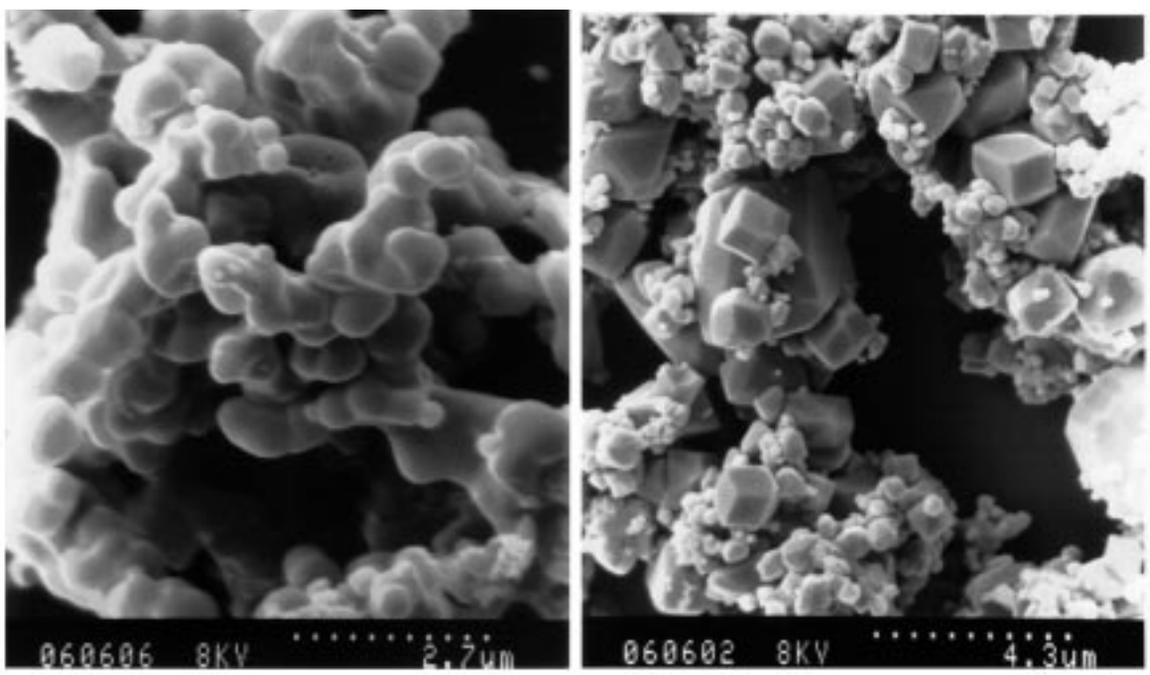

Fig. 1 The SEM images of (*a*) the amorphous black magnetic precipitate formed in ambient reactions and (*b*) magnetite formed hydrothermally (118 h, 200 °C)

also increases until with significant quantities of base the product is exclusively magnetite. Magnetite is also formed when base is present in the absence of any oxalate.

The reactions of iron(III) chloride are more complex (Tables 1 and 2). When base is present the product of the reactions at 200 °C is haematite (Table 1). It was also found that high-purity $Fe(ox)(H_2O)_2$ **2** can be produced in the reaction of iron(III) chloride with the disodium salt of oxomalonic acid in the absence of base or by starting from Fe_2O_3 and oxalic acid (Table 1). In the absence of base with sodium oxalate at 200 °C and below the iron is reduced giving $Fe(ox)(H_2O)_2$ **2** as the major product (with traces of magnetite) regardless of the order of addition of the various components (Table 2). At 240 °C the new mineral phase $Fe_2(ox)(OH)_2$ **1** forms, although as can be seen from Table 2 the order of addition of the components is crucial. Thus it is important to initiate hydrolysis of the iron(III) starting material by adding the oxalate only after the iron(III) chloride solution has stood for over 15 min. Otherwise as yet unidentified colourless crystals form.

Magnetite synthesis

The magnetite observed as an impurity in the iron oxalate phases was almost exclusively in a rhombic dodecahedral habit. A number of reactions were performed to investigate the morphology and particle size of hydrothermal magnetite. Key reactions are presented in Table 2. For iron(III) with a significant quantity of base the sole product is haematite, and the iron is not reduced. However, where little or no base is added, although $Fe(ox)(H_2O)_2$ **2** is formed as the major product, a small quantity of well crystallised magnetite is observed. Addition of base to aqueous iron(II) chloride gave small crystals of magnetite as the only product.

Scanning electron microscopy (SEM)

The SEM of the magnetic powder formed as a precipitate upon the addition of base to a mixed iron(II)–iron(III) solution showed it consisted of irregular shaped balls typically between 0.1 and 1 μm in diameter [Fig. 1(*a*)]. No evidence of crystal faces was seen, and indeed powder X-ray diffraction showed the sample to be amorphous. This is consistent with the idea that this rapid reaction produces nanoparticulate magnetite[19,21] which aggregates. These magnetic precipitates formed from mixtures of iron-(II) and -(III) starting materials under ambient conditions are obviously related to magnetite in some way, but are structurally difficult to define in a manner akin to the relationship between ferrihydrite and haematite. Similarly, magnetite produced hydrothermally (using $FeCl_2{\cdot}4H_2O$, $Na_2C_2O_4$, NaOH) with short reaction times (22 h at 200 °C) was also seen to consist of irregular balls (mostly about 1 μm) of presumably aggregated material. No evidence of crystallinity was observed.

However magnetite formed over a period of 100 h at 200 °C was found to be very much more crystalline [Fig. 1(*b*)].

Depending upon the reaction conditions, the size of the magnetite crystals can differ enormously. When magnetite is the sole product of the reaction the crystals are typically of the order of a few μm (after 100 h at 200 °C). If, however, the reaction is primarily giving $Fe(ox)(H_2O)_2$ **2**, a similar reaction time and temperature can give magnetite crystals of up to 0.15 mm in diameter. This difference in magnetite crystal size can simply be attributed to the relative supersaturation of the system and the number of nucleation sites for the formation of magnetite. When it is the sole product many more crystal nuclei are available for crystal growth. When magnetite is effectively the impurity only a few sites are available for growth and subsequently large crystals are formed.

In reactions producing the larger magnetite crystals we noted a rhombic dodecahedral habit. Although not unknown for magnetite, it is much more common to observe an octahedral morphology.[22] The relationship between an observed habit and crystal growth is a simple one; the observed faces are those which grow slowest. Our experiments show this preference for a rhombic dodecahedral habit (in the large crystals) can be attributed to the presence of the oxalate anion. In the synthesis of small magnetite crystals (Fe^{II} and base) SEM showed that with added oxalate the rhombic dodecahedral habit was seen to predominate, and although other habits were observed, like the truncated cube and octahedron, most of the truncation was of edges. The edge truncation of octahedra and cubes forms {011} and symmetry-related faces, the same as the faces in a rhombic dodecahedron.

Hydrolytic iron phases in nature

When considering the underlying chemistry of iron biomineral formation by organisms it is helpful to look first at the chemistry of terrestrial iron and its common mineral forms.[23–25] The oxygen-rich atmosphere of the Earth makes both Fe^0 and Fe^{II} unstable under normal conditions at the Earth's surface and they are oxidised to Fe^{III} to give various forms of iron(III) oxide, Fe_2O_3. The low solubility of these oxides means that iron cycling is dominated by solid transfer reaction with most of the iron in the form of suspended solids of finely divided particles. For example, only about 0.1 to 0.2% of the iron transported by rivers to the oceans is thought to exist in solution. Prior to the discovery by Lowenstamm[26] that magnetite can be produced biogenically it was believed that magnetite could not be formed under the temperatures and pressures found in the biosphere and that most of the magnetite observed in sediments arrived through solid transfer from igneous deposits. However, the relative stabilities of the +II and +III oxidation states of iron are such that only small deviations from 'normal' conditions can favour the oxidation of Fe^{II} to Fe^{III} or else the reduction of Fe^{III} to Fe^{II} with accompanying large changes in solubility. The underlying influences in this are the relative values of electrode (redox) potential, *E*, and pH; one a measure of the potential of electron activity, the other of the potential proton activity in the system. The value of *E* is found using the Nernst equation and thus the activities (sometimes approximated by concentrations) need to be taken into consideration. For metal ions these are often affected by the presence of co-ordinating species which can alter the electrode potential for oxidation or reduction through molecular orbital interactions (*e.g.* by changing the splitting of d orbitals in transition metals) or else overall pH through the release of protons into the medium, as, for example, in hydrolysis reactions. For iron in both terrestrial and biological contexts the available range of *E* and pH is governed by the stability range for water so that redox potentials which would either reduce or oxidise water need not be considered. However, these limits are dependent on both temperature and pressure as well as the concentration of iron.[27] A useful means of illustrating the stable forms of chemical species at various values of electrode potential, *E*, and pH is in a Pourbaix diagram.[24,25] Such plots reveal that at low potentials and pH values Fe^{II} is quite stable giving iron in a highly soluble form, whereas at pH values around the physiological and normal environmental levels Fe^{III} predominates in the form of insoluble oxyhydroxide species unless the conditions are highly reducing. In the region between pH 5 and 9 the interplay between the two oxidation states depends critically on the balance between pH and *E*. This has ensured that iron-dependent biology has been able to accommodate the change in the Earth's atmosphere from reducing to oxidising through the development of systems capable of tuning electrode potentials and local pH to favour the required oxidation state. It is exactly this fine-tuning which the use of hydrothermal methods can reproduce.

Phase control in the iron oxalate system

Iron oxyhydroxide and oxide phases all result from the hydrolysis reactions of iron ions.[28–30] Either Fe^{II} or Fe^{III} can be used as starting material for the production of iron(III) oxyhydroxide and oxide minerals.[30] Hydrolysis of iron(III) leads to the highly insoluble iron(III) 'hydroxide' as an initial solid product which forms immediately on addition of a base to an aqueous solution of iron(III) salt. This material is usually formulated as '$Fe(OH)_3$' and called ferrihydrite, but its exact composition is highly variable and it is highly likely that it is metastable and corresponds to a mixture of oxyhydroxide phases of various degree of hydration. The presence of anions such as chloride, phosphate or sulfate can also influence the nature of the phase formed.[28] Depending on how this material is treated, different well defined oxyhydroxide and oxide phases can be stabilised. If '$Fe(OH)_3$' is left to age under water, the two well defined AX_2-type iron(III) oxyhydroxide phases, lepidocrocite, γ-FeO(OH), and goethite, α-FeO(OH), can be formed. An alternative route to the formation of these is *via* the iron(II) hydroxide, $Fe(OH)_2$, which has the CdI_2 structure, exemplified for hydroxides by the mineral brucite, $Mg(OH)_2$.[30] The transformation of a layered brucite structure, $M(OH)_2$ into a three-dimensional MO(OH) structure such as goethite results from removal of half the hydroxide protons and a relative shift of the metal layers to optimise the sharing of the remaining protons between the layers. Goethite, the α phase, can be further transformed by heating into the related iron(III) oxide haematite, α-Fe_2O_3. These α-phase minerals possess hexagonally close-packed arrays of oxygen atoms (from the oxides and hydroxides) with iron centres in the octahedral holes. The γ-phase minerals, γ-FeO(OH) and γ-Fe_2O_3, are based on cubic close-packed structures, again with the iron centres in octahedral holes. Maghaemite, γ-Fe_2O_3, is a defect structure, which, under ambient conditions, only forms *via* the mixed-valence phase magnetite. In fact, the structure of γ-Fe_2O_3 is not very well defined, but can be understood by considering the oxidation of the iron(II) centres in wüstite, $Fe^{II}O$, which has the sodium chloride structure, but with an Fe : O ratio of less than unity. The charge imbalance is corrected through oxidation of some of the iron(II) centres, ultimately leading to magnetite [with a cubic inverse spinel structure with iron(II) ions and half the iron(III) ions in octahedral sites and the remaining iron(III) ions in tetrahedral sites[30]] and then γ-$Fe^{III}_2O_3$. Thus the relationships of the iron(III) oxyhydroxide and their oxide minerals to their iron(II) counterparts is clear.

The phases likely to be important in the iron oxalate system are iron oxide, hydroxide and oxyhydroxide of both Fe^{II} and Fe^{III} and phases incorporating the templating oxalate ligand. The phases we observe are structurally related which allows us to rationalise the way in which the templating oxalate ligand can influence the morphology of the magnetite crystals produced in these reactions. It would appear that under the hydrothermal

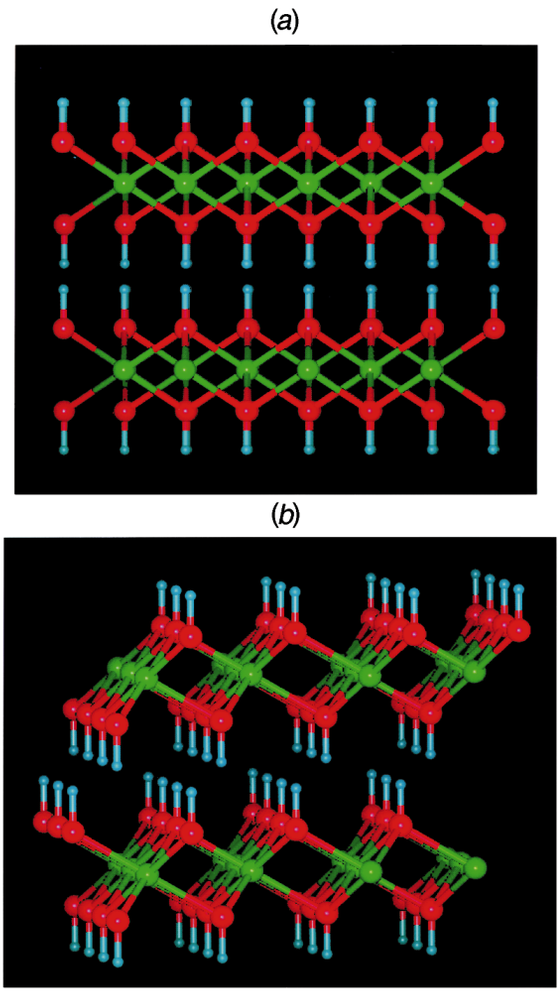

Fig. 2 Two views of brucite perpendicular to the three-fold axis; magnesium green, oxygen red, hydrogen blue

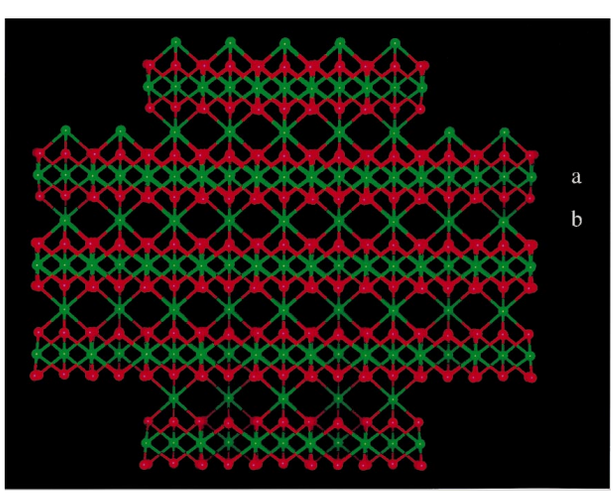

Fig. 3 View of the octahedral iron atoms in magnetite perpendicular to the three-fold axis along [110]; iron green

conditions we have used in the presence of oxalate the iron(II) oxidation state is stabilised even if the starting material is Fe^{III}. This can be understood as a modification to the Pourbaix diagram for the system, since under ambient conditions the nature and identity of the products are different. As we have pointed out previously[8–10,13,31] the brucite structure tends to be an important component of hydrolytically produced phases. This structure is exemplified for Fe^{II} as $Fe(OH)_2$ and consists of layers of hexagonally close packed μ_3-hydroxides with the metal centres in the octahedral holes to give sheets of edge-sharing

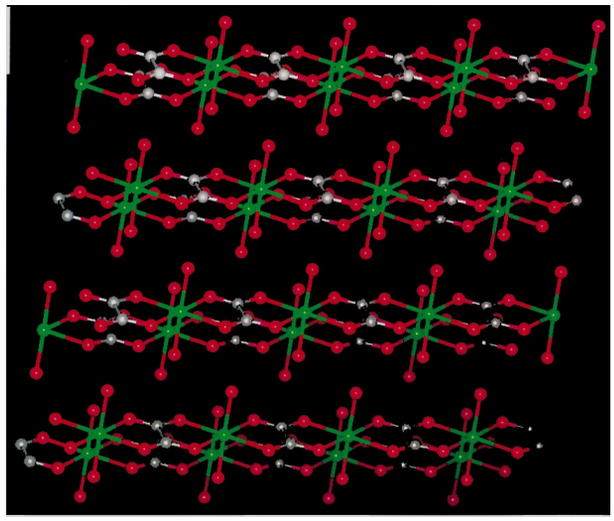

Fig. 4 Side-on view of the iron oxalate chains in humboldtine, $Fe(ox)(H_2O)_2$; carbon grey

$M(OH)_6$ octahedra. Within the crystal lattice these layers are arranged so that hydrogen bonding is optimised through the interdigitation of the μ-$_3$hydroxide groups from adjacent layers (Fig. 2). The relationship between this and magnetite can be seen if we consider the octahedral iron ions (a mixture of Fe^{II} and Fe^{III}) in magnetite only (Fig. 3). Now layers of FeO_6 edge-sharing octahedra (marked a in the figure) are linked through further rows of octahedral iron centres (row b). As we have shown, when oxalate is present it is possible to isolate hydrolytic phases containing oxalate or to produce magnetite with altered crystal morphology. Two different but related oxalate phases can be isolated from hydrothermal reactions. The compound $Fe(ox)(H_2O)_2$ is a recognised mineral, humboldtine, found in brown coal deposits in, for example, Bohemia and Bavaria.[32] Its structure consists of hydrogen-bonded chains with the octahedrally co-ordinated iron(II) centres bridged by chelating oxalate ligands, each co-ordinated to two iron centres. The co-ordination sphere of each iron centre is completed by two *trans* water ligands and it is these which form the hydrogen-bonded array of chains (Fig. 4). This mineral is also easily prepared under ambient conditions unlike the new phase $Fe_2(ox)(OH)_2$ which formally results from the loss of oxalic acid and two water molecules from a dinuclear unit of $Fe(ox)(H_2O)_2$, equation (1). These two oxalate phases can also be described

$$2Fe(ox)(H_2O)_2 \longrightarrow Fe_2(ox)(OH)_2 + H_2ox + 2H_2O \quad (1)$$

in terms of the hydrolytic products of general form $[M_yL_zO_p(OH)_q(H_2O)_r]^b$ where, for $Fe(ox)(H_2O)_2$, M = Fe^{II}, $b = 0$, $y = 1$, $z = 1$, $p = 0$, $q = 0$, $r = 2$ and for $Fe_2(ox)(OH)_2$, M = Fe^{II}, $b = 0$, $y = 2$, $z = 1$, $p = 0$, $q = 2$, $r = 0$.

The crystal structure of $Fe_2(ox)(OH)_2$ **1** also contains chains of iron centres linked by bridging and chelating oxalates but now each oxalate ligand co-ordinates to four iron(II) centres (Fig. 5), a reflection of the formal loss of one oxalate per two iron centres. The asymmetric unit of **1** consists of one iron, one hydroxide and half an oxalate ligand. The iron atom is bonded to three (meridional) hydroxides, a chelating oxalate and a monodentate oxalate but the environment is greatly distorted from octahedral, with bond angles ranging from 73.68(8) to 120.58(1)°. The bond lengths are all reasonable for Fe^{II} and range from 2.060(2) to 2.264(2) Å with the bonds to hydroxides being the shortest, followed by those to the chelating oxalate and the monodentate oxalate having the greatest Fe–O length. The oxalate ligand bridges four iron atoms in a *trans*-chelating/monodenate fashion [Fe(1)···Fe(1A) 3.370(1) Å] in the same way as observed in Fe(ox)[33] and the bond lengths and angles within the ligand are all normal. The hydroxide bridges between

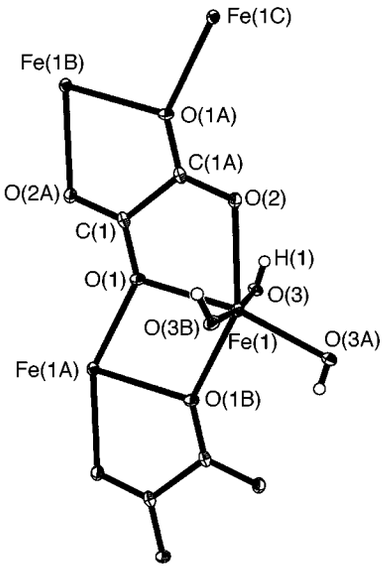

Fig. 5 View of a portion of the structure of $Fe_2(ox)(OH)_2$ showing the atom numbering scheme with thermal ellipsoids drawn at 50% probability. Selected bond lengths (Å): Fe(1)–O(1) 2.194(2), Fe(1)–O(2) 2.264(2), Fe(1)–O(3) 2.091(2), Fe(1)–O(1B) 2.157(2), Fe(1)–O(3A) 2.060(2), Fe(1)–O(3B) 2.146(2), C(1)–O(1) 1.262(4), C(1)–O(2A) 1.249(4), C(1)–C(1A) 1.544(6)

three iron atoms and has a flattened pyramidal geometry with the sum of the Fe–O–Fe angles coming to 345.6° in comparison to 328.5° expected for the apex of a tetrahedron. The Fe_3 triangle centred on the hydroxide has sides of length 3.233(1), 3.638(1) and 3.709(1) Å. Each iron atom is bridged *via* one oxygen atom to six other identical atoms which make up a distorted hexagonal array reminiscent of the brucite, $Mg(OH)_2$, structure (Fig. 6). The relationship to the brucite structure is made clear by comparing Fig. 6(*b*) and 6(*c*). In Fig. 6(*b*) the brucite structure is presented with adjacent pairs of μ_3-OH removed. Comparison of this framework with that of the iron hydroxide framework of $Fe_2(ox)(OH)_2$ **1**, *i.e.* with the oxalate removed, reveals the close relationship of their topologies. In the brucite lattice the metal atoms all lie within a plane whereas in **1** there is puckering of the iron sheet. Neighbouring iron hydroxide layers are held together by oxalate linkers so that the overall structure can be viewed as $Fe(OH)_2$ which has been modified by replacement of one hydroxide by half an oxalate ligand (Fig. 7). Fig. 8 shows that edge-sharing hydroxide-bridged dinuclear units are linked in zigzag chains *via* oxalate bridges. Adjacent chains are linked *via* the μ_3-OH bridges. This structure can also be compared with that of magnetite. If we again view the magnetite structure in terms of the octahedral iron centres alone (Fig. 3) we can imagine replacing the *b* iron rows with oxalate linkers as is shown in the alternative view of $Fe_2(ox)(OH)_2$ (Fig. 7). This sheds light on the action of oxalate in directing the crystal morphology as observed in our experiments. Viewing the magnetite structure, again showing only the octahedral iron sites, as the {011} plane (Fig. 9) reveals that the *a* rows lie in strips running parallel to the [101] direction. The large square channels in the figure contain the tetrahedral iron centres in the complete crystal structure. The distance between iron centres in adjacent strips is 5.94 Å which compares with 5.80 and 5.93 Å between iron centres in adjacent brucite-like layers in $Fe_2(ox)(OH)_2$. Clearly, in the structure of $Fe_2(ox)(OH)_2$, oxalate anions are interspersed between such layers, suggesting that the interaction of oxalate at the growing surface {011} and symmetry-equivalent planes in magnetite blocks the tetrahedral iron site and is responsible for the observed rhombic dodecahedral morphology.

This control over magnetite morphology echoes that observed in biological systems which utilise magnetite as a

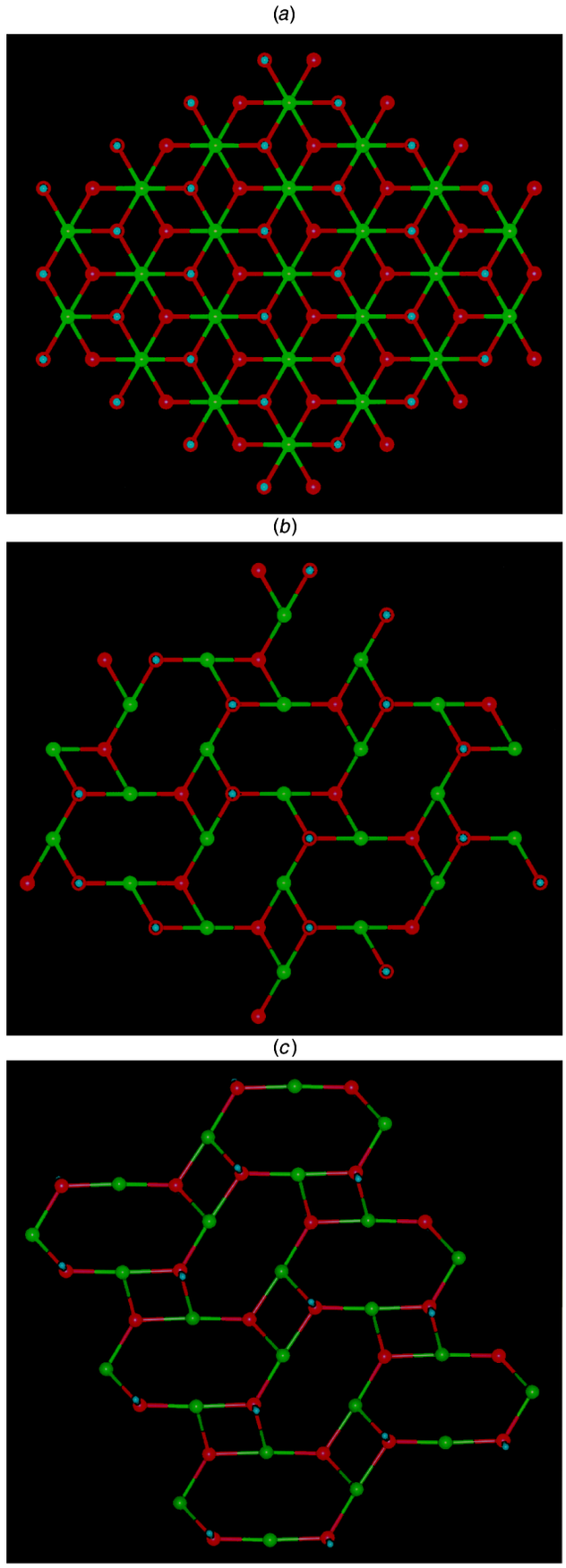

Fig. 6 The relationship of $Fe_2(ox)(OH)_2$ to the brucite structure. (*a*) View of the hexagonal array present in the brucite structure, (*b*) view of the brucite array with adjacent pairs of bridging hydroxides removed and (*c*) the iron hydroxide framework of $Fe_2(ox)(OH)_2$ omitting the oxalate linkers

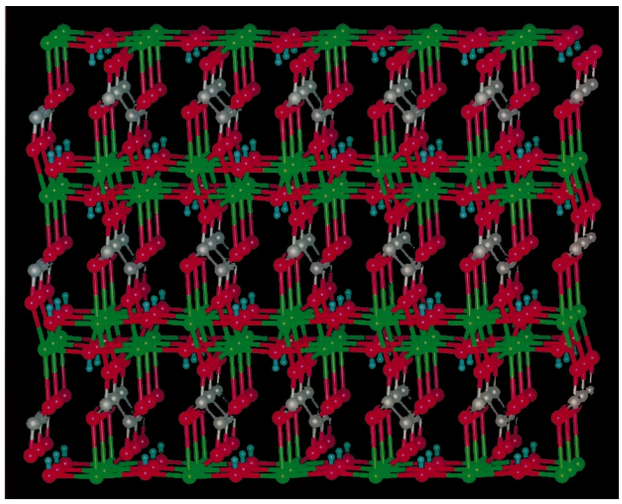

Fig. 7 Packing diagram showing the three-dimensional structure of $Fe_2(ox)(OH)_2$

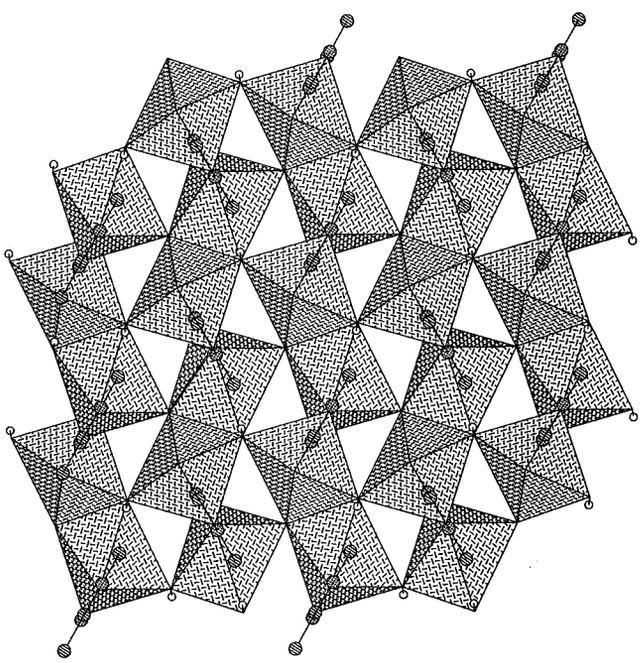

Fig. 8 Polyhedral representation of a layer in $Fe_2(ox)(OH)_2$

sensor. Magnetotactic bacteria are the most widely studied group of creatures using magnetite in this way, although other organisms such as salmon are known to use magnetite for navigational purposes. Studies on single crystals of magnetite found in such bacteria reveal an elongation along the easy axis of magnetisation [111] direction and crystal morphologies of cuboctahedra, cubic, elongated cubic shapes (rectangular) and elongated rhombic dodecahedra (truncated hexagonal prisms) as well as bullet-shaped crystals related to the hexagonal prisms have been observed.[34] So far, no morphologies corresponding to the commonly observed octahedra found in ambient syntheses of magnetite have been seen.

The effect of oxalate on redox potential

Our experiments show that in the absence of oxalate in basic media the products from hydrothermal syntheses reflect the oxidation state of the iron starting material. If Fe^{III} is used the major product is haematite, for Fe^{II} it is magnetite. This can be understood from Pourbaix diagrams which indicate that iron(III) oxides and magnetite are the most stable forms at high pH values. As noted before, such diagrams are temperature and pressure dependent so that hydrothermal conditions can favour

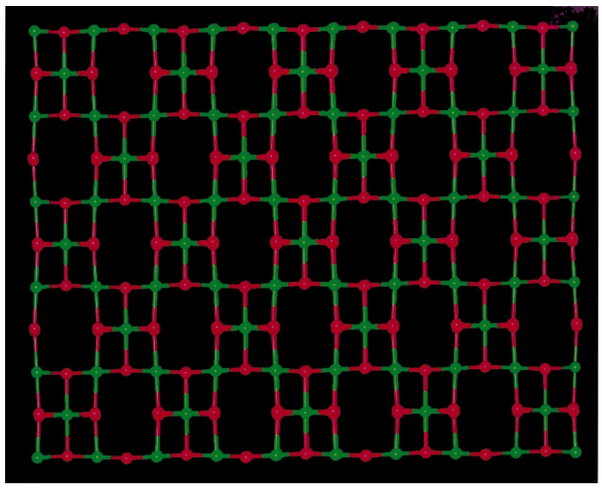

Fig. 9 View of the {011} plane showing only the octahedral iron sites in magnetite

the stabilisation of different oxidation states from those observed under ambient conditions. When oxalate is also present the oxidation state of the iron and the identity of the product(s) is critically dependent on the amount of base present. Thus, with no or small amounts of base, starting from both Fe^{II} and Fe^{III} the oxalate phases contain iron exclusively in the +II state. This is likely to be a consequence of the change in E for the Fe^{III}–Fe^{II} couple in the presence of oxalate (compare, $E^{\ominus} = 0.771$ V for Fe^{III}–Fe^{II} in pure water with values such as $E^{\ominus} = 0.020$ V in the presence of oxalate). As the amount of base is increased, the formation of magnetite is also observed until with large amounts of base oxalate is no longer incorporated in the iron-containing product and the results are the same as those for which no oxalate is present except for the changed morphologies of the crystals of the iron oxide phases.

Conclusion

Hydrothermal synthetic methods can be used to mimic the ability of nature to manipulate mineral phase morphology in bimineralisation processes. We have been able to demonstrate that using hydrothermal conditions the oxalate template can direct crystal morphology in reactions producing magnetite as well as influence the oxidation state of the iron. In addition, we have been able to produce two oxalate-containing phases, one of which, $Fe_2(ox)(OH)_2$, has not been observed previously and thus probably represents a metastable mineral form, modelling another aspect of biomineralisation processes; the stabilisation of unusual mineral phases. The structure of this mineral also sheds light on possible ways in which the oxalate template can direct the morphology of magnetite crystals.

References

1 S. Mann, *J. Chem. Soc.*, *Dalton Trans.*, 1997, 3953.
2 G. A. Ozin, *J. Chem. Soc.*, *Dalton Trans.*, 1997, 3941.
3 S. Mann and G. A. Ozin, *Nature* (*London*), 1996, **382**, 313.
4 B. R. Heywood and S. Mann, *Chem. Mater.*, 1994, **6**, 311.
5 D. Walsh and S. Mann, *Nature* (*London*), 1995, **377**, 320.
6 D. Walsh and S. Mann, *Chem. Mater.*, 1996, **8**, 1944.
7 R. B. Frankel, *Iron Biominerals*, eds. R. B. Frankel and R. P. Blakemore, Plenum, New York, 1990, p. 1.
8 S. L. Heath and A. K. Powell, *Angew. Chem.*, *Int. Ed. Engl.*, 1992, **31**, 191.
9 A. K. Powell, S. L. Heath, D. Gatteschi, L. Pardi, R. Sessoli, G. Spina, F. Del Giallo and F. Pieralli, *J. Am. Chem. Soc.*, 1995, **117**, 2491.
10 S. L. Heath and A. K. Powell, *Comments Inorg. Chem.*, 1994, **15**, 255.
11 C. J. Harding, R. K. Henderson and A. K. Powell, *Angew. Chem.*, *Int. Ed. Engl.*, 1993, **32**, 570.
12 S. O. H. Gutschke, M. Molinier, A. K. Powell, R. E. P. Winpenny and P. T. Wood, *Chem. Commun.*, 1996, 823.

13 S. O. H. Gutschke, M. Molinier, A. K. Powell and P. T. Wood, *Angew. Chem.*, *Int. Ed. Engl.*, 1997, **36**, 991.
14 TEXSAN Structure Analysis Software, Molecular Structure Corporation, Houston, TX, 1992.
15 G. M. Sheldrick, SHELXTL PLUS, Siemens Analytical X-Ray Instruments, Madison, WI, 1990.
16 G. M. Sheldrick, SHELXL 93, Program for Crystal Structure Refinement, University of Göttingen, 1993.
17 J. Hugget, *Liebigs. Ann. Chem.*, 1929, **10**, 445.
18 T. Kanzaki and T. Katsura, *J. Chem. Soc.*, *Dalton Trans.*, 1986, 1243.
19 F. Mazzi and C. Garavelli, *Period. Mineral.*, 1957, **26**, 269.
20 R. Deyrieux and A. Peneloux, *Bull. Soc. Chim. Fr.*, 1969, **8**, 2675.
21 T. Adschiri, K. Kanazawa and K. Arai, *J. Am. Ceram. Soc.*, 1992, **75**, 1019.
22 T. Dubois and G. Demazeau, *Mater. Lett.*, 1994, **19**, 38.
23 P. O'Neill, *Environmental Chemistry*, Chapman and Hall, London, 2nd edn., 1993.
24 K. B. Krauskopf and D. K. Bird, *Introduction to Geochemistry*, McGraw-Hill, New York, 3rd edn., 1995.
25 R. M. Garrels and L. Christ, *Solutions, Minerals and Equilibria*, Harper and Row, New York, 1965.
26 H. A. Lowenstamm, *Bull. Geol. Soc. Am.*, 1962, **13**, 435.
27 A. Rabenau, *Angew. Chem.*, *Int. Ed. Engl.*, 1985, **24**, 1026.
28 C. M. Flynn, *Chem. Rev.*, 1984, **84**, 31.
29 W. Schneider and B. Schwynn, *Aquatic Surface Chemistry*, ed. W. Stumm, Wiley, New York, 1987, p. 167.
30 A. F. Wells, *Structural Inorganic Chemistry*, Oxford University Press, London, 3rd edn., 1962.
31 S. L. Heath, P. A. Jordan, I. D. Johnson, G. R. Moore, A. K. Powell and M. Helliwell, *J. Inorg. Biochem.*, 1995, **59**, 785.
32 P. Ramdohr and H. Strunz, *Klockmann's Lehrbuch der Mineralogie*, Ferdinand Enke Verlag, Stuttgart, 1967 p. 757.
33 Yu. D. Kondrashov, V. S. Bogdanov, S. N. Golubev and G. F. Pron, *Zh. Strukt. Khim.*, 1985, **26**, 90.
34 S. Mann and R. B. Frankel, *Biomineralization. Chemical and Biological Perspectives.*, eds. S. Mann, J. Webb and R. J. P. Williams, VCH, Weinheim, 1989, p. 389.

Received 23*rd June* 1997; *Paper* 7/04400C